Molecular Cell, Vol. 18, 109–121, April 1, 2005, Copyright ©2005 by Elsevier Inc. DOI 10.1016/j.molcel.2005.03.005

GR and HMGB1 Interact Only within Chromatin and Influence Each Other's Residence Time

Alessandra Agresti,[1] Paola Scaffidi,[1,4] Alberto Riva,[3] Valeria R. Caiolfa,[1,5,*] and Marco E. Bianchi[2,5,*]
[1]San Raffaele Research Institute
[2]San Raffaele University
Via Olgettina 58
20132 Milano
Italy
[3]Children's Hospital Informatics Program
Harvard Medical School
300 Longwood Avenue
Boston, Massachusetts 02115

Summary

Most nuclear proteins reside on a specific chromatin site only for seconds or less. The hit-and-run model of transcriptional control maintains that transcription complexes are assembled in a stochastic fashion from freely diffusible proteins; this contrasts to models involving stepwise assembly of stable holo complexes. However, the chances of forming a productive complex improve if the binding of one factor promotes the binding of its interactors. We prove here that in living cells, the glucocorticoid receptor and HMGB1 interact only within chromatin and not in the nucleoplasm and decrease each other's mobility. Thus, the formation of a GR-HMGB1-chromatin complex is more likely than one would expect from independent binding to chromatin of GR and HMGB1. Remarkably, this complex is potentially stable, and its disassembly is effected by active, ATP-consuming processes. We propose that kinetic cooperativity among transcription factors in chromatin binding may be a common feature in transcription and DNA transactions.

Introduction

Our knowledge of the identity and of the roles of the transcription factors, cofactors, and chromatin-modifying activities is reasonably advanced. However, the dynamic process by which these proteins interact on DNA to activate transcription is poorly understood; although we know the cast and a general description of the play, we ignore the script.

Two paradigms dominate our thinking: the well-established enhanceosome model (Carey, 1998; Merika and Thanos, 2001) and the relatively more novel idea that most protein-DNA and protein-protein interactions in the nucleus are very dynamic and highly reversible (Misteli, 2001).

The enhanceosome model is based on the concept of context-dependent interactions among transcription factors, which promote their cooperative assembly on DNA and endow the complex with exceptional stability. This is compatible with the high affinity of NF-κB for its DNA binding sites within the interferon-β enhancer (the model enhanceosome) and follows naturally from considerations on the physicochemical equilibria between multiple interacting macromolecules. In fact, in vitro measurements confirm the stability of the enhanceosome, and chromatin immunoprecipitation (ChIP) experiments suggest a stepwise recruitment of proteins to a slowly accreting complex (Agalioti et al., 2000; Lomvardas and Thanos, 2001; Munshi et al., 2001).

Although highly successful in explaining the specificity of transcriptional control, and theoretically intuitive, the classical enhanceosome model clashes with the observation that transient and dynamic binding is a common property of all chromatin proteins with the exception of core histones. Glucocorticoid receptor (GR) has been particularly well studied: GR binds and unbinds to chromatin in cycles of only a few seconds (McNally et al., 2000); remarkably, such fleeting interactions are sufficient to promote large-scale remodeling of chromatin lasting a few hours and to correlate with transcriptional activation (Muller et al., 2001). In this "hit-and-run" model, transcriptional activation reflects the probability that all components required for activation will meet at a certain chromatin site (McNally et al., 2000).

We believe that the concept of interaction-dependent stabilization of the complex, central to the enhanceosome paradigm, can apply to transient interactions as well. Stability and affinity are thermodynamic concepts that are related to the amount of free energy liberated during complex assembly, and there is no direct constraint on the time frame involved in the interaction. There is however an indirect constraint: affinity is defined as the ratio between the on rate (binding) and the off rate (unbinding); thus, if affinity increases, either the on rate becomes faster or the off rate becomes slower (or both). These rates can be fast (as in a hit-and-run model) or slow (as in a classical enhanceosome model); it is the change in their ratio that brings about a change in stability.

These basic thermodynamic considerations lead to a prediction: each protein in a complex should influence the binding kinetics of its partners, even in a hit-and run scenario. We tested this kinetic prediction by analyzing the physical interaction of HMGB1 (high mobility group box 1 protein) with GR in living cells. Two results stand out that we believe can be generalized to the majority of transcription factors: (1) the two interacting proteins affect each other's residence time on chromatin, and (2) the interaction has a preferential physical location on the regulatory regions of genes.

HMGB1 is a major component of mammalian chromatin and is endowed with an "architectural" function:

*Correspondence: bianchi.marco@hsr.it (M.E.B.); caiolfa.valeria@hsr.it (V.R.C.)
[4]Present address: Cell Biology of Gene Expression, National Cancer Institute, National Institutes of Health, 41 Library Drive, Building 41, Bethesda, Maryland 20892.
[5]These authors contributed equally to this work.

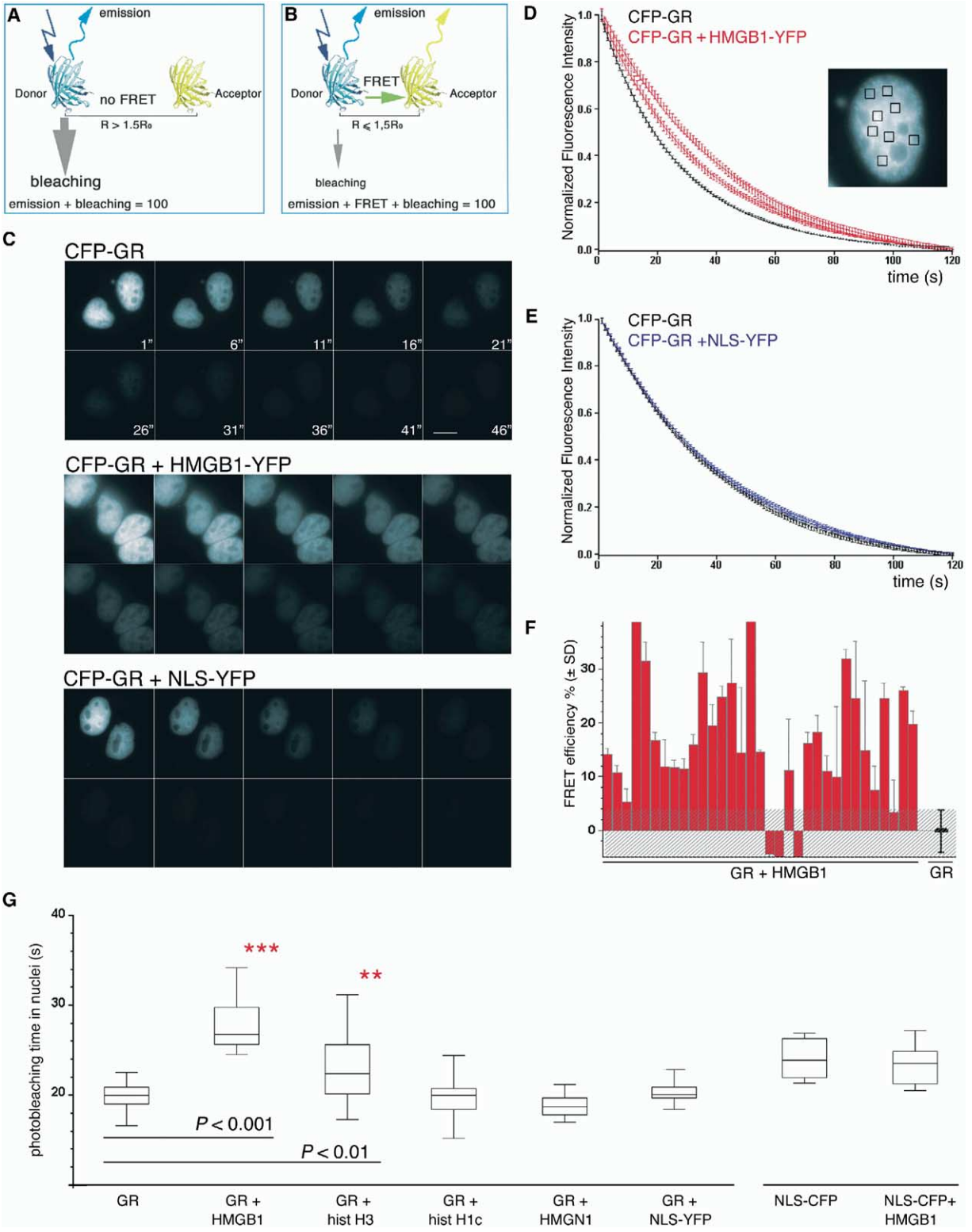

Figure 1. pbFRET Shows that HMGB1 and GR Interact in Living Cells

(A and B) FRET and photobleaching. R_0 is the Förster radius, the distance between donor and acceptor at which FRET efficiency is 50% (about 5 nm for the CFP-YFP pair). When donor and acceptor are separated by 2 R_0, FRET efficiency is reduced to only 1.6%. For this reason, FRET provides an excellent way of establishing whether molecules interact.

(B) If FRET occurs, the time spent by donor molecules in the excited state decreases, and therefore the probability of photobleaching is reduced. Thus, photobleaching of the donor will take longer.

it binds within the minor groove of DNA and bends the double helix to facilitate the formation of multiprotein complexes (reviewed in Agresti and Bianchi, 2003). HMGB1 is probably the most mobile nuclear protein: each and every HMGB1 molecule roams the nucleus in a few seconds (Phair et al., 2004b; Scaffidi et al., 2002). The interaction between GR and HMGB1 has been demonstrated functionally by transfection assays, and by genetics: *Hmgb1*$^{-/-}$ thymocytes survive dexamethasone-induced apoptosis because GR activity is blunted by the absence of HMGB1; however, the GR-HMGB1 complex may be too dynamic for biochemical detection: EMSAs show that HMGB1 promote GR binding to DNA, but they do not resolve GR-HMGB1-DNA ternary complexes; moreover, in vitro reconstitution of GR binding to chromatin is not affected by HMGB1 (Boonyaaratanakornkit et al., 1998; Melvin et al., 2002; Calogero et al., 1999; Fletcher et al., 2002).

We followed the interaction between GR and HMGB1 in living cells via FRET (fluorescence resonance energy transfer), by tagging them with Cyan (CFP) and Yellow Fluorescent Protein (YFP), respectively. Mutants of HMGB1-YFP and CFP-GR that cannot bind chromatin show no FRET, indicating that chromatin (as opposed to the nucleoplasm) is the site of the GR-HMGB1 interaction. Moreover, FRET occurs efficiently between HMGB1-YFP and CFP-GR on arrays of MMTV promoters; this indicates that the interaction occurs on GR binding sites that are part of functioning promoters. We then show that GR is more mobile in cells that are devoid of HMGB1, as we predicted. When cells are depleted of ATP, the difference in GR mobility between *Hmgb1*$^{-/-}$ and wild-type cells is greatly increased, indicating that the cooperation between HMGB1 and GR in extending each other's residence time on chromatin is actively counterbalanced by catalyzed, ATP-requiring disassembly processes.

Results

Fluorescently Tagged GR and HMGB1

We tagged GR and HMGB1 with the well-known GFP variants, CFP and YFP (Tsien, 1998). The resulting fusion proteins are in all respects equivalent to HMGB1-GFP and to GFP-GR, which were previously shown to be transcriptionally active and equivalent to the unmodified cellular proteins (Htun et al., 1996; Muller et al., 2001; Pallier et al., 2003; Scaffidi et al., 2002). To check for the specificity of the interaction between GR and HMGB1, we also used tagged histone H3 (Kimura and Cook, 2001), histone H1c, and HMGN1 (Misteli et al., 2000). In addition, we prepared NLS-CFP and NLS-YFP, in which a canonical Nuclear Localization Signal (NLS) was cloned at the N terminus of CFP and YFP (Bonaldi et al., 2003).

It is very difficult to obtain stable cell clones expressing HMGB1, either unmodified or GFP tagged; therefore, we transfected cells transiently. We first used HEK293 cells because these cells do not express GR constitutively, and thus, after transfection, they express a population of CFP-GR molecules undiluted by native GR. Figure S1 (in the Supplemental Data available with this article online) shows living HEK cells cotransfected with the various expression vectors. Cells grown in glucocorticoid-free medium contain CFP-GR in the cytoplasm (data not shown); treatment for 10 min with dexamethasone, a synthetic GR ligand, induces CFP-GR nuclear translocation. CFP-GR is then distributed in the whole nucleus with the exclusion of nucleoli and heterochromatic regions; HMGB1-YFP is distributed in the whole nucleus. Control proteins NLS-YFP and NLS-CFP prevalently have a nuclear localization and their presence does not alter GR and HMGB1 distribution.

Donor Photobleaching Kinetics

Within living cells, protein-protein interactions can be analyzed by FRET. FRET is a process in which energy is transferred from a fluorophore in the excited state (donor) to another fluorophore (acceptor) in the ground state. The transfer efficiency varies inversely with the 6th power of the donor-acceptor separation over the range of 1–10 nm. In practice, FRET between CFP and YFP occurs efficiently only at distances below 7 nm, about the size of a typical protein (Patterson et al., 2000; Figure 1B). Thus, FRET can be used as a "spectroscopic ruler" to detect contacts between proteins (Sekar and Periasamy, 2003).

We were able to detect FRET between CFP-GR and HMGB1-YFP by sensitized emission, which visualizes

(C) Sequential donor photobleaching is achieved by illuminating living cells through CFP filters. A stack of 120 images, 1 s exposure each, is acquired. The gallery shows 1 image every 5 s. Already at raw image level, it is evident that HMGB1-YFP protects CFP-GR from photobleaching. The scale bar represents 10 μm.

(D) Inset: small areas of 400 pixels (ROIs, squares) are defined on the stack of images, and average photobleaching kinetics are calculated as described in Experimental Procedures. Red curves represent photobleaching kinetics in two different cells cotransfected with CFP-GR and HMGB1-YFP; the error bars represent the standard deviation within the same cell. The black curve represents the average photobleaching kinetics of 7 cells transfected with CFP-GR alone.

(E) Blue curves represent photobleaching kinetics in two different cells cotransfected with CFP-GR and NLS-YFP, the black curve is the same as in panel (D). Error bars represent the standard deviation within the same cell. The curves are superimposable, indicating that FRET does not occur.

(F) Each bar represents FRET efficiency in a single nucleus (calculated as described in Experimental Procedures); error bars represent the standard deviation within the same cell. Data are pooled from three experiments in different days. The gray area represents the 95% confidence limit around 0% FRET efficiency (calculated from GR alone cells): cells falling within this area are not considered to show FRET between CFP-GR and HMGB1-YFP.

(G) Synopsis of representative results. In the "box-and-whiskers" graphs, the base and the top of the box indicate the 25th and 75th percentile, the line within the box the 50th percentile, and the whiskers extend to the highest and lowest measurements. The only statistically significant differences are between CFP-GR alone and CFP-GR+HMGB1-YFP (***, $p < 0.001$), and between CFP-GR alone and CFP-GR+H3-YFP (**, $p < 0.01$).

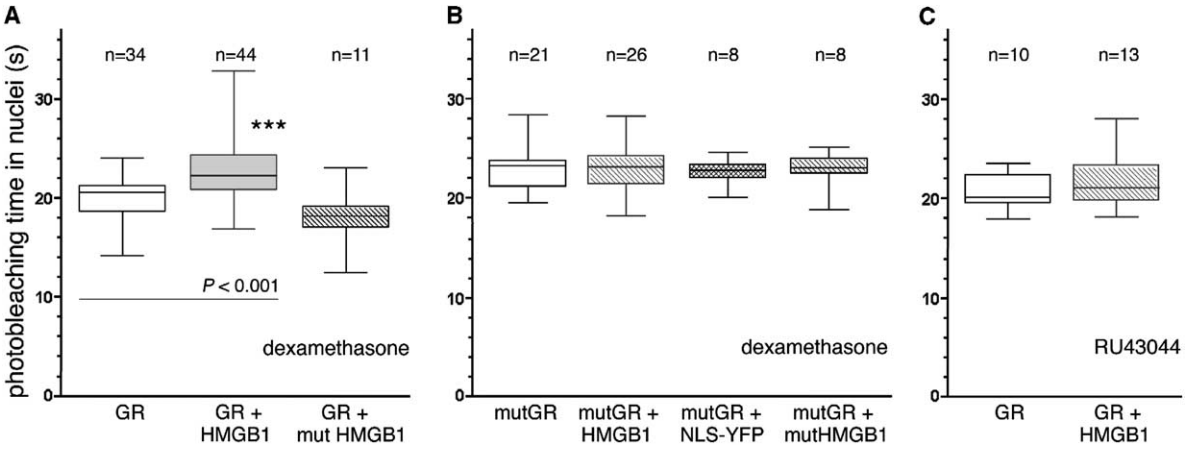

Figure 2. DNA Binding-Incompetent GR and HMGB1 Do Not Interact with Wild-Type Partners or between Each Other

Box-and-whiskers representation is described in the Figure 1 legend.

(A) 3T3 fibroblasts were cotransfected with CFP-GR and either wild-type or mutHMGB1-YFP. Photobleaching times of CFP-GR alone and CFP-GR + mutHMGB1-YFP do not differ significantly, indicating that HMGB1 not bound to chromatin does not interact with GR.

(B) Similar experiments were done with the GR A477T mutant. Photobleaching times of donor alone and with wild-type HMGB1 do not differ significantly, indicating that GR not bound to DNA does not interact with HMGB1. Mutant GR and mutant HMGB1 also do not interact. The photobleaching time of mutant CFP-GR is different from that of wild-type CFP-GR, because of the exquisite sensitivity of the spectral properties of CFP to the chemical environment.

(C) Singly and doubly transfected cells were exposed to RU43044, a glucocorticoid antagonist that inhibits GR DNA binding without interfering with dimerization and nuclear transport. The photobleaching times of CFP-GR alone and CFP-GR + HMGB1-YFP do not differ significantly, indicating once again that GR must bind to DNA in order to interact with HMGB1.

the simultaneous decrease of CFP fluorescence and increase of YFP fluorescence (data not shown). However, CFP photobleached significantly during the time required for imaging; for this reason, we followed the interaction by using donor photobleaching FRET microscopy (pbFRET), which relies on the fact that energy transfer to the acceptor protects the donor against photobleaching (Clegg, 1996; Jovin and Arndt-Jovin, 1989). Photobleaching is an irreversible photochemical conversion of a fluorophore in the excited state into a different nonfluorescent molecular species. If FRET occurs, the time spent by donor molecules in the excited state decreases, and the probability of donor photobleaching is reduced. Thus, photobleaching of the donor will take longer (Figure 1B). pbFRET is convenient for detecting FRET between CFP and YFP fusion proteins in transiently transfected in living cells because it is insensitive to absolute fluorescence (Jovin and Arndt-Jovin, 1989; Young et al., 1994; Figure S2).

We measured pbFRET as shown in Figure 1C. HEK293 cells transfected either with the donor alone (CFP-GR) or together with an acceptor (HMGB1-YFP or NLS-YFP) were imaged in a wide-field microscope at the specific donor wavelengths, every second for 2 min, until CFP fluorescence was reduced to background levels. We then quantified the donor fluorescence intensity in stacks of 120 images. In the example given in Figure 1D (inset), we designated random "regions of interest" (ROI) in a given nucleus (squares) and computed the fluorescence intensity of each area as a function of illumination time. Photobleaching intensities were analyzed as described in Experimental Procedures.

The red curves in Figure 1D represent mean photobleaching kinetics of single nuclei from two individual cells coexpressing CFP-GR and HMGB1-YFP. It can be noted that both cells differ from the total population of cells transfected with CFP-GR alone. In the control experiment (Figure 1E), the "CFP-GR + NLS-YFP" curves (blue) overlapped the "CFP-GR" curve (black). These results indicate that HMGB1-YFP is closer than 7 nm to CFP-GR, but not to NLS-YFP.

Figure 1F shows the FRET efficiency (calculated as indicated in Experimental Procedures) in individual living cells in different experiments over several days. FRET is somewhat variable, and in a few cells undetectable, because of the variability in the concentration ratio between donor and acceptor. This underscores the necessity of statistical evaluation of results.

Photobleaching kinetics allow the calculation of a "photobleaching time" (the time at which 50% of the initial fluorescence is destroyed, see Experimental Procedures). Populations of cells can be visualized in a "box-and-whiskers" graph (Figure 1G), which shows the highest and lowest measurements together with the twenty-fifth, fiftieth, and seventy-fifth percentile. The HEK cells expressing CFP-GR alone ("GR") cluster around a photobleaching time of 20 s, and those expressing CFP-GR and HMGB1-YFP ("GR+HMGB1") cluster around 27 s. The difference is statistically highly significant ($p < 0.001$). GR plus histone H3-YFP clusters around 22 s, which is also significantly different from GR alone ($p < 0.01$); this is expected because GR binds to GREs within an assembled nucleosome (Perlmann and Wrange, 1988) and thus within a short distance of a core histone like H3. The photobleaching times of the other controls (GR plus NLS-YFP, HMGN1-YFP, and histone H1c-YFP) are not different from that of GR alone.

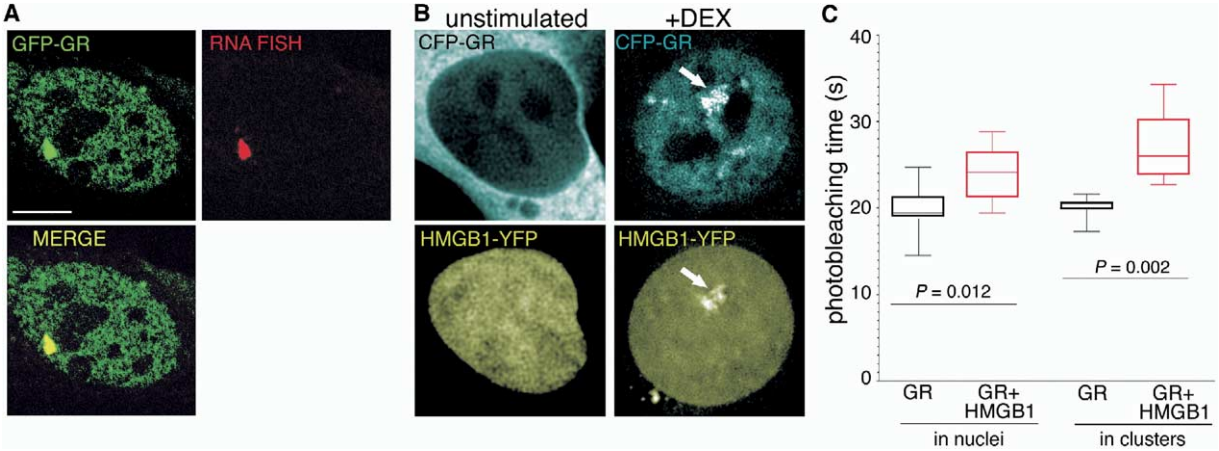

Figure 3. HMGB1 Interacts with GR on the MMTV Array

(A) Mouse 3134 cells, containing the MMTV array, were transfected with GFP-GR, stimulated with dexamethasone, fixed, and subjected to RNA fluorescent in situ hybridization with a probe to MMTV transcripts. A bright green cluster of GFP-GR molecules and the nascent transcripts colocalize (confocal imaging, the scale bar represents 5 μm).

(B) 3134 cells were cotransfected with HMGB1-YFP and CFP-GR. Prior to dexamethasone treatment, GR was located in the cytoplasm, and HMGB1 was evenly distributed in the nucleus. After dexamethasone exposure, HMGB1-YFP coclustered with CFP-GR (arrows).

(C) FRET occurs between CFP-GR and HMGB1-YFP in the MMTV cluster: nine whole cells expressing CFP-GR alone or CFP-GR and HMGB1-YFP were illuminated; we then analyzed donor photobleaching kinetics within the nuclear area containing the cluster, or within randomly chosen ROIs in the rest of nucleus. Box-and-whiskers representation is described in the legend to Figure 1.

The absence of FRET indicates that other chromatin proteins do not come in contact with a significant fraction of GR molecules, and neither does a protein that is free in the nucleoplasm. This is particularly significant for histone H1, which is even more abundant than HMGB1; chance encounters due to the sheer abundance of chromatin proteins are thus excluded.

We also tested a different donor: NLS-CFP (soluble in the nucleoplasm), which does not come within FRET distance to a significant fraction of HMGB1-YFP molecules. Note that NLS-CFP has a photobleaching time (22 s) different from CFP-GR (20 s). This is due to the sensitivity of GFP derivatives to the chemical environment, such as the protein to which they are fused (Chattoraj et al., 1996), and highlights the importance of evaluating FRET by comparison with the appropriate control donor.

We next used pbFRET to analyze protein-protein interactions in mouse 3T3 fibroblasts, which express GR naturally. Since GR is a dimer, the molecular species $(GR)_2$, $(CFP\text{-}GR)_2$, and CFP-GR/GR should all be present in transfected 3T3 cells at relative concentrations that differ from cell to cell depending on the expression level of the CFP-GR transgene. Indeed, in 3T3 cells, the difference in the photobleaching time of CFP-GR in the presence and absence of HMGB1-YFP is smaller than in HEK293 cells, and the fraction of cells where FRET occurs with marginal efficiency is higher (Figure S3). However, the difference is highly significant statistically ($p < 0.001$), indicating that pbFRET can be used in any cell type.

Taken together, these results show that CFP-GR and HMGB1-YFP touch each other inside the nucleus of living cells.

Binding to DNA Is Mandatory for GR-HMGB1 Interactions

The experiments described previously indicate that HMGB1 and GR interact in the nucleus of dexamethasone-stimulated cells, but no information is provided about where the two proteins meet. There are three possibilities: GR and HMGB1 associate (1) in the nucleoplasm, (2) on DNA, or (3) in both places. To distinguish between these scenarios, we explored whether one or both proteins need DNA binding in order to get in touch.

HMG boxes are characterized by hydrophobic residues in conserved positions that anchor the protein to the DNA minor groove (Thomas and Travers, 2001). We then substituted three intercalating residues with alanines; Figure S4 shows that the triple-mutated HMGB1-YFP (mutHMGB1-YFP) still localizes in the nucleus but does not bind to chromatin. Fluorescence recovery after photobleaching (FRAP) experiments indicate that mutHMGB1-GFP is much more mobile than HMGB1-GFP (see ahead, Figure 6), almost as much as NLS-GFP, which is thought to diffuse freely within the nucleus without interacting with other macromolecules (data not shown).

New experiments were set up in which CFP-GR was the donor as before and mutHMGB1-YFP was the acceptor (Figure 2A). Whereas wild-type HMGB1-YFP protected GR-CFP from photobleaching, mutHMGB1-YFP did not. Therefore, HMGB1 must bind DNA in order to form a complex with GR.

We next tested the interaction between HMGB1 and a GR mutant that is unable to bind DNA. The well-characterized mutation A458T in the second zinc finger (D loop) of the human GR DNA binding domain (GR-DBD) prevents dimerization and DNA binding (Reichardt et

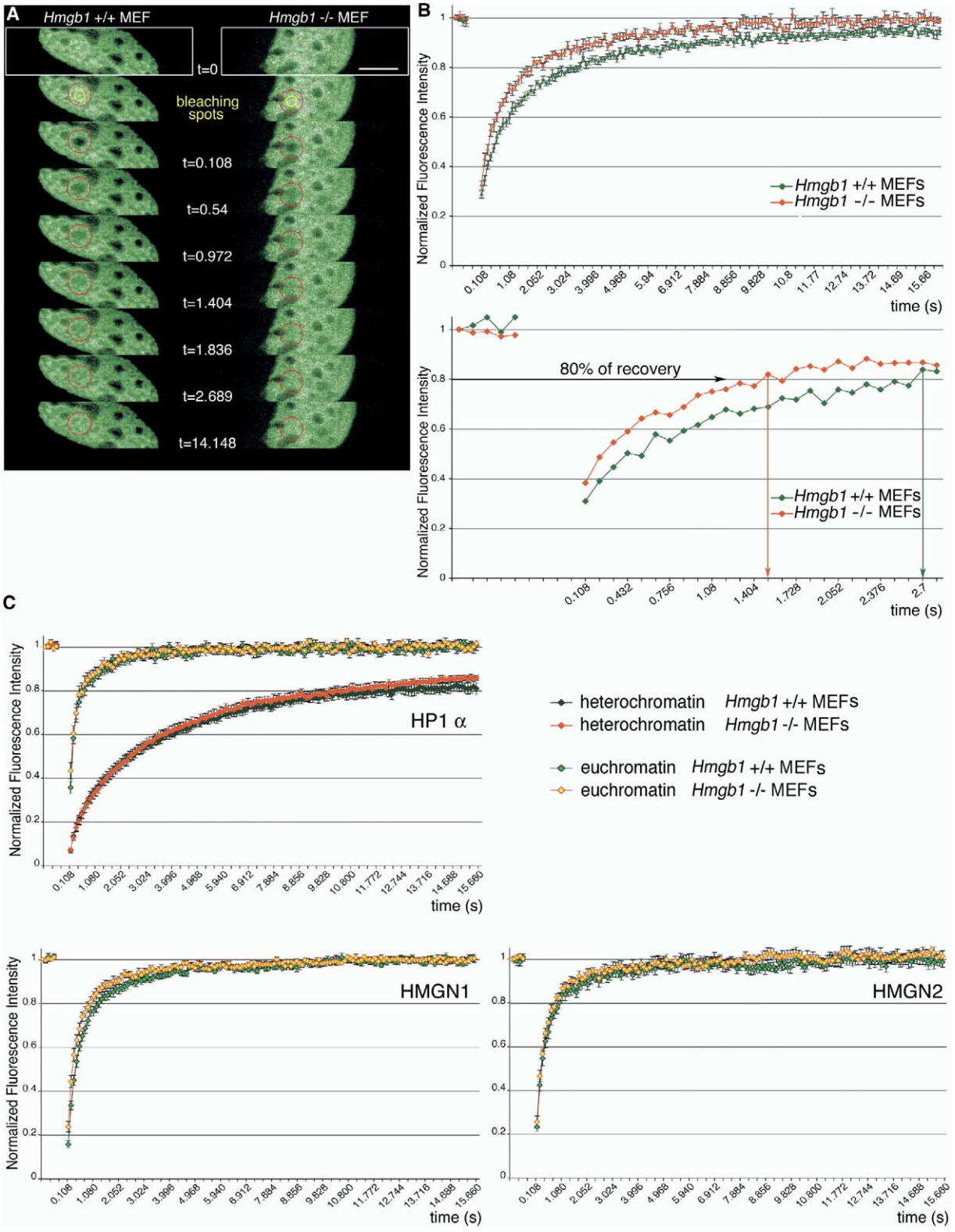

Figure 4. GR Shows Increased Mobility in *Hmgb1*$^{-/-}$ MEFs As Compared to *Hmgb1*$^{+/+}$ MEFs

(A) Time-lapse imaging of GFP-GR before and during recovery after photobleaching in *Hmgb1*$^{+/+}$ (left) and knockout (–/–) (right) MEFs. White contours indicate the real size of images. Yellow circles indicate the bleaching areas, and the red contours are only to highlight the interesting area. Images shown are from a stack of 150 images collected every 108 ms; 14 s is representative of very late times. The scale bar represents 10 μm.

al., 1998). We then introduced the equivalent mutation (A477T) in our rat CFP-GR construct. MutCFP-GR translocated to the nucleus upon dexamethasone stimulation and its nuclear distribution was identical to that of CFP-GR (Figure S4A). HMGB1-YFP did not protect mutCFP-GR from photobleaching, in contrast to the protection given to wild-type CFP-GR (compare Figures 2B and 1G). Thus, GR also needs to bind DNA in order to meet HMGB1. Significantly, mutHMGB1-GFP also failed to protect mutCFP-GR from photobleaching (Figure 2B), indicating that the two proteins do not interact in the nucleoplasm.

The synthetic glucocorticoid antagonist RU43044 has been reported to block GR binding to DNA without interfering with dimerization and nuclear transport (Belikov et al., 2001). HMGB1-YFP cannot protect RU43044-loaded CFP-GR from photobleaching (Figure 2C).

Taken together, these data strongly support the notion that both GR and HMGB1 must be bound to DNA in order to interact with each other, and disprove the possibility that the interaction may occur in the nucleoplasm.

Both GR and HMGB1 Bind to MMTV Arrays

To verify that the interaction of GR and HMGB1 occurs on GR binding sites, we took advantage of a mouse cell line (3134) that contains a tandem array of the mouse mammary tumor virus promoter (the MMTV array; McNally et al., 2000). After transfection with GFP-GR and dexamethasone addition, a brightly fluorescent chromatin area is visible where a large number of GFP-GR molecules bind to GREs within the MMTV array (Figure 3A). The same brightly fluorescent area contains a large number of transcripts originating from the MMTV array, as shown by RNA fluorescence in situ hybridization (Muller et al., 2001, and Figure 3A). Thus, the MMTV array is transcriptionally active.

It is well-known that the transcribing MMTV array also attracts fluorescently tagged GR-interacting molecules, like GRIP-1 (Becker et al., 2002). Sure enough, the GR-bright clusters were also HMGB1-bright (Figure 3B). Interestingly, we were unable to detect HMGB1-bright areas in the nuclei of cells not stimulated with dexamethasone. This indicates that the distribution of HMGB1 is directly affected by the distribution of GR.

Although conditional colocalization is a good indication of interaction, we positively tested whether CFP-GR and HMGB1-YFP were within FRET distance on the MMTV array. Whole 3134 cells transfected with CFP-GR alone or with both CFP-GR and HMGB1-YFP were illuminated, and we compared photobleaching times both on the cluster and on unrelated areas in the nucleus (Figure 3C). FRET was very clearly detected in every single cluster in CFP-GR + HMGB1-YFP cells, whereas FRET in nondescript areas of the nucleus was statistically demonstrable but much less evident. Transfection with mutHMGB1-YFP did not alter the photobleaching times of CFP-GR on the clusters (data not shown).

The Mobility of GR Increases in *Hmgb1*$^{-/-}$ Cells

The experiments described previously indicate that HMGB1, GR, and chromatin form a ternary complex. To test directly the notion that the formation of a complex with HMGB1 increases the stability of GR on chromatin, we transfected GFP-GR into wild-type and *Hmgb1*$^{-/-}$ primary embryonic fibroblasts (MEFs), derived from 14-day mouse embryos, and performed FRAP experiments (Figure 4A). Reproducibly, GFP-GR was more mobile in *Hmgb1*$^{-/-}$ cells than in *Hmgb1*$^{+/+}$ cells (Figure 4B). A recovery of 80% was achieved in 2.7 ± 0.3 s in wild-type MEFs (n = 10) against 1.5 ± 0.1 s in *Hmgb1*$^{-/-}$ MEFs (n = 11, $p < 0.005$, two representative curves are shown in Figure 4C).

In principle, GR mobility could change in *Hmgb1*$^{-/-}$ cells both because of the specific interaction of HMGB1 with GR or because of a global alteration in the organization of chromatin due to the absence of HMGB1. In fact, HMGB1 has a role in the maintenance of global genome stability (Giavara et al., 2005). We then tested the mobility of other nuclear proteins: HP1-α and HMGN2 have identical mobility in wildtype and knockout (–/–) cells; HMGN1 is slightly more mobile in knockout cells, but the variation is much smaller than in the case of GR (Figure 4C). We conclude that although the absence of HMGB1 can have an effect on the global organization of chromatin and on the mobility of some nuclear proteins, the variation in GR mobility is mainly due to its specific interaction with HMGB1.

Catalyzed, ATP-Dependent Processes Limit the Lifetime of GR-HMGB1-Chromatin Complexes

Recent data indicate that a significant fraction of GR turnover on its binding sites is not driven by chemical equilibria but is rather a steady-state condition that requires energy consumption. We then measured the mobility of GFP-GR in *Hmgb1*$^{-/-}$ and wild-type cells depleted of ATP. A fraction of GR became immobile in ATP-depleted wild-type cells, and the rate of fluorescence recovery in the bleached spot also became slower (Figure 5A). This indicates that the mobile GR fraction is faster in unperturbed cells as compared to ATP-depleted cells, as reported (Stavreva et al., 2004). Tellingly, the GR immobile fraction was much smaller in *Hmgb1*$^{-/-}$ than in wild-type cells, and the mobile GR

(B) FRAP analysis of GFP-GR in *Hmgb1*$^{+/+}$ (green dots) and *Hmgb1*$^{-/-}$ MEFs (orange dots). Upper graph: dots indicate mean values, and error bars indicate standard error, from 10 cells of a representative experiment. Lower graph: an enlargement of the recovery kinetics of two cells closest to the mean of their group, in order to show calculation of 80% recovery. Recovery is faster in knockout cells than in wild-type cells: 80% recovery is reached in 2.7 and 1.4 s respectively (t test; n = 10; $p < 0.005$); complete recovery in knockout cells is reached in 9 s, while it is beyond 16 s in wild-type cells.

(C) Fluorescence recovery in wild-type and *Hmgb1*$^{-/-}$ MEFs of control chromatin proteins. The mobility of HP1α is very different in euchromatin and heterochromatin, and both mobilities are shown; HMGN1 and HMGN2 do not have substantially different mobilities in euchromatin and heterochromatin (data not shown). Dots indicate mean values, and bars standard error, from seven cells of a representative experiment.

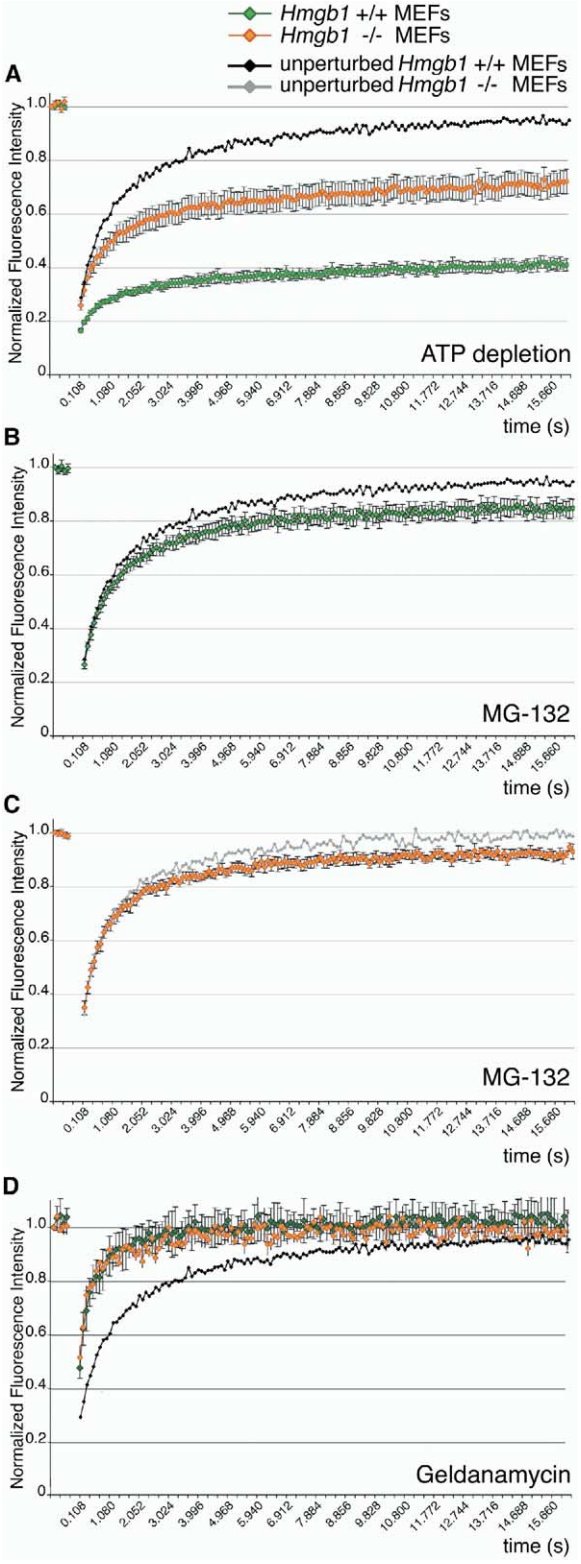

Figure 5. GR Mobility Is Very Different in *Hmgb1*$^{+/+}$ and *Hmgb1*$^{-/-}$ MEFs under Perturbed Conditions

The mobility of GR in unperturbed cells is redrawn from Figure 4 for easy comparison as a thin black line (wild-type cells) or a thin gray line (*Hmgb1*$^{-/-}$ cells). Dots indicate mean ± standard error from 10 cells of a representative experiment.

(A) ATP depletion (treatment with deoxyglucose and sodium azide for 30 min) leads to a significant decrease of GR mobility in *Hmgb1*$^{+/+}$ MEFs (green curve) as compared to *Hmgb1*$^{-/-}$ MEFs (orange curve); the immobile fraction is also much smaller in knockout cells.

(B and C) Qualitatively similar results are obtained after treatment with the proteasome inhibitor MG-132 (10 μM) for 2 hr of wild-type (B) and *Hmgb1*$^{-/-}$ cells (C).

(D) GR mobility increases when wild-type and *Hmgb1*$^{-/-}$ cells are incubated with 2.5 μg/ml geldanamycin, an inhibitor of the Hsp90 chaperone. Note that in this case there is no difference in GR mobility between the two cell types.

fraction was faster (compare the slopes of the curves at early time points). We conclude that HMGB1 extends considerably the stability of GR on the chromatin of ATP-depleted cells. On the other hand, the same data show that energy-dependent processes dissociate both GR-HMGB1-chromatin complexes and GR-chromatin complexes; the net result is that in unperturbed cells HMGB1 slows down the turnover of GR only by a limited amount because active processes enforce a limitation on the maximum time spent by GR on chromatin.

Several mechanisms have been implicated in the cycling of GR on chromatin, including molecular chaperones, nucleosome remodelling machineries, and the proteasome (Freeman and Yamamoto, 2002; Elbi et al., 2004; Stavreva et al., 2004; Nagaich et al., 2004). All of these consume ATP and could be affected by ATP depletion. We first focused on the proteasome: in wild-type cells, the inhibitor MG-132 immobilized a fraction of GR and reduced the mobility of the rest, as reported (Stavreva et al., 2004, and Figure 5B); the fraction of immobilized GR was clearly smaller in *Hmgb1*$^{-/-}$ cells, and the overall recovery rate of fluorescence was higher (Figure 5C). Again, this argues that the stabilizing effect of HMGB1 on GR binding is counteracted by the disassembly processes that depend on proteasome activity. We then tested geldanamicyn, an inhibitor of Hsp90: geldanamycin increased GR mobility in wild-type cells (Figure 5D), confirming a previous suggestion that chaperones promote GR assembly rather than disassembly (Stavreva et al., 2004). In the presence of geldanamycin there was almost no difference in GR mobility between *Hmgb1*$^{-/-}$ and wild-type cells (Figure 5C), suggesting that the Hsp90 chaperone and HMGB1 are required together for the same mechanistic process.

We also tested whether the mobility of HMGB1 itself could be at least partially energy dependent. In this experiment, we used *Hmgb1*$^{-/-}$ cells because there would be no interference from endogenous HMGB1 in these cells. The entire pool of HMGB1-GFP was mobile when ATP was available (Figure 6A), but a quantitatively minor but significant amount of protein (about 2%) became immobile in ATP-depleted cells (Figure 6B). In addition, the recovery in the photobleached area was statistically slower, even if by a very small amount, in ATP-depleted cells when compared to unperturbed cells. The mobility of mutHMGB1 is very similar in unperturbed and ATP-depleted cells (compare Figures 6A and 6B). Differences in HMGB1 mobility in cells treated with MG-132 and geldanamycin were small and statistically nonsignificant (results not shown).

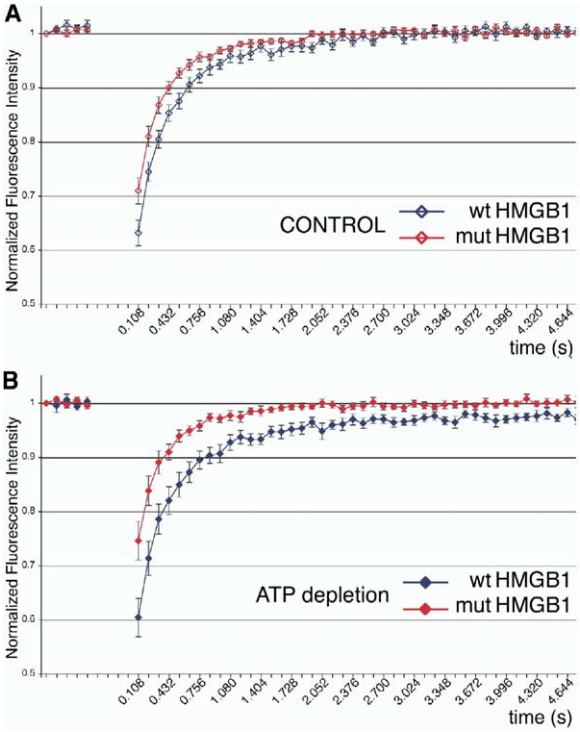

Figure 6. HMGB1 Mobility Is at Least Partially Energy Dependent

Hmgb1$^{-/-}$ MEFs were transfected with either wild-type or mutated HMGB1. Dots indicate mean ± standard error from 10 cells of a representative experiment.

(A) Fluorescence recovery of wild-type HMGB1 in unperturbed living cells is extremely fast (blue curve); mutated HMGB1 recovers even faster (red curve), indicating reduced, if not absent, interactions. Full recovery is reached in approximately 2 and 3 s, respectively. No immobile fraction is apparent for both proteins.

(B) Upon ATP-depletion, wild-type HMGB1 shows a small but reproducible immobile fraction (2%–3%); mutHMGB1 behaves like in unperturbed cells, and there is no detectable immobile fraction.

Discussion

We have shown in living cells that HMGB1, a chromatin architectural protein, and GR, a transcription factor, cooperate in controlling transcription by increasing each other's residence time on chromatin. Moreover, their interaction occurs on DNA and is not appreciable in solution within the nucleus, i.e., in the nucleoplasm. In particular, the interaction between HMGB1 and GR occurs on the GR binding sites in functioning promoters. However, the complex formed is far from stable in living cells; indeed, the complex lifetime appears to be actively curtailed by ATP-consuming processes.

HMGB1 and GR: A Complex Difficult to Hold

HMGB1 is an important player in nuclear transactions because it is very abundant (about 1,000,000 molecules) in most mammalian cells, is extremely conserved between species, and *Hmgb1* KO mice are not viable. HMGB1 interacts with nucleosomes and with many transcription factors, facilitating their binding to naked DNA and chromatin (Agresti and Bianchi, 2003). GR has been shown to interact with HMGB1 by means of EMSAs on naked DNA, by reporter assays, and because *Hmgb1*$^{-/-}$ thymocytes become insensitive to dexamethasone-induced apoptosis (Boonyaaratanakornkit et al., 1998; Calogero et al., 1999). However, ternary complexes between HMGB1, DNA, and steroid receptors cannot be isolated biochemically. This may be due to the specific dynamic nature of the interaction of HMGB1 with steroid receptors because its interaction with a viral transcription factor is indeed stable (Ellwood et al., 2000).

We have established the existence of HMGB1-GR complexes within the nuclei of living cells by using pbFRET, a robust technique that measures the bleaching of the donor fluorophore (CFP) rather than the sensitized emission of the acceptor (YFP). More specifically, we have shown that fluorescently tagged GR molecules are within FRET distance (<7 nm) of fluorescently tagged HMGB1. This contiguity appears to be due to a true interaction and not by random encounter, since a nuclearly located YFP (NLS-YFP) does not show evidence of FRET with CFP-GR, and CFP-GR does not interact with other chromatin proteins, such as histone H1 fused to YFP; these controls also exclude the possibility that CFP and YFP are brought together by their small but detectable tendency to dimerize (Tsien, 1998). Seven nanometers is about the diameter of a typical protein, and we can safely deduce that tagged GR and HMGB1 form a complex. Since both GFP-GR and HMGB1-GFP behave like their untagged counterparts (McNally et al., 2000; Pallier et al., 2003), we deduce that GR and HMGB1 also interact.

GR Interacts with HMGB1 within Chromatin, and Not in the Nucleoplasm

A GR mutant that does not bind DNA does not interact with wild-type HMGB1, nor does an HMGB1 mutant that does not bind DNA interact with wild-type GR. In fact, the GR mutant and the HMGB1 mutant do not interact even though they are both soluble in the nucleoplasm, excluding the possibility that the mutant/wild-type combinations do not encounter each other because they are confined to different phases (soluble nucleoplasm versus chromatin). We also show that in living cells, after stimulation with dexamethasone, HMGB1-YFP congregates on the MMTV array, and on the cluster, FRET with CFP-GR can be readily observed.

We thus conclude that chromatin provides the appropriate environment for the interaction between GR and HMGB1, and that at least a part of the interaction occurs on GR binding sites in functioning promoters.

The Interaction between HMGB1 and GR Prolongs the Residence Time of Both on Chromatin

We directly proved that GR is approximately 2-fold more mobile in *Hmgb1*$^{-/-}$ cells, implicating that the interaction with HMGB1 tethers it to chromatin for a longer time. The effect of HMGB1 on GR might be quite large, but it is partially masked by limitations on the lifetime of the complex that living cells enforce actively.

GR turnover on chromatin is at least partially a catalyzed, energy-consuming process. In ATP-depleted cells, a fraction of GR becomes immobile, and the mo-

bile fraction gets slower (Stavreva et al., 2004). The dependence of GR mobility on the presence of HMGB1 is much less evident in unperturbed cells as compared to cells with low ATP levels; this suggests that many of the potentially stable GR-HMGB1-chromatin complexes are continually disassembled by active, ATP-consuming processes. A large difference between wild-type and *Hmgb1*$^{-/-}$ cells is also visible when the proteasome is inhibited.

Several investigators have suggested that GR binds to a separate functional compartment of the nucleus, termed nuclear scaffold, after the perturbation of ATP levels or of the proteasome. The binding to the nuclear scaffold cannot be visualized as a different subnuclear distribution of GR, and it is dependent on the presence of GR's DNA binding domain (Schaaf and Cidlowski, 2003); thus, binding to the scaffold might not be mechanistically very different from binding to active chromatin. We show that HMGB1 mobility is reduced, and a small fraction of HMGB1 molecules (about 2%) become immobile, when ATP is depleted, suggesting that HMGB1 follows the fate of GR (and may be tethered to it). The magnitude of these effects are consistent with the fact that HMGB1 is 50–100 times more abundant than GR, and therefore most HMGB1 molecules might be unaffected.

Kinetic Cooperativity in Promoter Binding

Our results indicate that GR and HMGB1 do affect each other's probability of binding to chromatin. In our view, the key elements are the locale and the timing.

The fact that HMGB1 and GR interact only on chromatin introduces a very significant concentration effect: chromatin binds reversibly both HMGB1 and GR, and it acts as a catalyst surface for the formation of the complex. The time domain of the interaction is seconds: the complex assembles fast and disassembles fast. The disassembly kinetics is determined by catalyzed, ATP-consuming processes, which probably impose the same limit to the lifetime of every complex present on chromatin (or at least in the same chromatin domain where the activities reside). If the GR disassembly kinetics is set by external processes, then the overall change in GR mobility must be due to a change in the assembly kinetics: GR binds faster to its binding sites in the presence of HMGB1 than in its absence. Geldanamycin, an inhibitor of the Hsp90 chaperone, increases GR mobility in both wild-type and *Hmgb1*$^{-/-}$ cells and eliminates the difference between these cells: this suggests that HMGB1 facilitates GR assembly like Hsp90. A possible functional interaction between Hsp90 and HMGB1 should be addressed by further experiments.

In conclusion, we have taken a feature of the enhanceosome model—the interaction of several proteins endows the complex with increased thermodynamic stability—and tested whether it would be compatible with a hit-and-run model. We found that this is indeed the case: the kinetics of GR depends to a considerable extent on the presence of its interactor HMGB1. Thus, the principles of combinatorial interactions and complex stability apply to hit-and-run models even if the complex itself has a very limited lifetime. The same kinetic effects should apply to all transcription factors that interact on particular DNA sites.

Experimental Procedures

Expression Vectors

Plasmid HMGB1-YFP contains the open reading frame of HMGB1 fused at the 5′ end of the coding region of the enhanced yellow fluorescent protein (pEYFP, Clontech) and was generated as previously described (Scaffidi et al., 2002). CFP-specific point mutations (pECFP sequence, Clontech) were introduced in the rat GFP-GR vector (kindly provided by T. Grange). NLS-CFP and NLS-YFP were prepared as described for NLS1-GFP (Bonaldi et al., 2003). Plasmids expressing tagged HMGN1 and –N2 were kindly provided by M. Bustin; human HP1α and histone 1c, by T. Misteli; histone H3, by H. Kimura. HMGB1-YFP was used as template to generate the triple mutant in four-step PCR mutagenesis, using as external primers: 5′HMG-GFP (5′-ATCCTCGAGACATGGGCAAAGGAG-3′) and 3′HMG-GFP (5′-ACCCCGCGGTTCATCATCATCATC-3′) and three pairs of internal mutagenic primers (substitutions in bold type): 37Phe forward (5′-CTTCTGTCAAC**GCA**TCAGAGTTTTC-3′), 37Phe reverse (5′-GAAAACTCTGA**TGC**GTTGACAGAAG-3′); 15Phe forward (5′-CTTCGGCCTTC**GCA**TTGTTCTGTTC-3′), 15Phe reverse (5′-GAACAGAACAA**TGC**GAAGGCCGAAG-3′); 34Ile forward (5′-CTGGCTTATCC**GCA**GGTGATGTTG-3′), 34Ile reverse (5′-CAACAT CACC**TGC**GGATAAGCCAG-3′).

Plasmid CFP-GR was used as template to generate the A477T mutant in rat GR (corresponding to A458T of mouse GR) in two-step PCR mutagenesis, using as external primers: BsrGI forward (5′-ATCACTCTCGGCATGGACG-3′) and BsrGI reverse (5′-GTTT GTACAGTAAAAGCTATAAATTC-3′) and a pair of internal mutagenic primers (substitutions in bold type): A477T forward (5′-CAATT ACCTTTGT**A**CTGGAAGAAACGATTGC-3′), A477T reverse (5′-CGT TTCTTCCAGTACAAAGGTAATTGTGCTG-3′).

Cell Lines, Transfections, and Stimulation with Dexamethasone or RU43044

All cell lines, including *Hmgb1*$^{-/-}$ and wild-type mouse embryonic fibroblasts (MEFs) (Calogero et al., 1999), were grown in DMEM plus 10% fetal bovine serum (FBS, Gibco), 100 IU/ml penicillin, and 100 μg/ml streptomycin, in a 5% CO_2 humidified atmosphere. For transfection, 10^5 cells were plated on glass-bottom petri dishes (MatTek Corporation, Ashland, MA). After 16 hr, the culture medium was replaced with fresh phenol red-free medium containing glucocorticoid-depleted FBS (charcoal/dextran-treated FBS, Hyclone). Three hours later, cells were transfected with FuGene (Roche) and 1 μg plasmid DNA. For cotransfection, we defined conditions that produced approximately the same fluorescence intensity of both donor and acceptor. Cells were analyzed 18–20 hr posttransfection and after 20 min stimulation with 100 nM dexamethasone (Fluka). When required, instead of dexamethasone, RU43044 (a gift of Orjan Wrange) was added to cells at 1 μM for 60 min. RNA FISH was performed according to Muller et al. (2001).

Wide-Field Imaging

Living cells were stained with 0.5 μg/ml Hoechst 33342 for 10 min at 37°C. Blue (Hoechst 33342), cyan (CFP), and yellow (YFP) fluorescent images were acquired with Olympus 100×/1.4 NA Plan Apo or oil immersion objective lenses on a DeltaVision Restoration Microscopy System (AppliedPrecision, Issaquah, WA) built around an Olympus IX70 microscope equipped with mercury-arc illumination. Twenty images spaced by 0.4 μm on the z axis were collected with a Coolsnap_Hq/ICX285 CCD camera (Photometrix, Tucson, AZ) and deconvolved by the constrained iterative algorithm available in the SoftWoRx 2.50 package (AppliedPrecision) using 10 iterations and standard parameters. Each image measured 512 × 512 effective pixel size 0.062 μm. Filters (Hoechst 33342: Ex360/40, Em457/50; CFP: Ex436/10, Em470/30, dichroic 86002bs; YFP: Ex500/20, Em535/30; dichroic 86002v1) are from Chroma Technology Corp. (Brattleboro, VT).

pbFRET

Sequential donor photobleaching was carried out with our Olympus/DeltaVision system by illuminating living cells in DMEM plus

30 mM HEPES (pH 7.6), 1% FCS and 100 nM dexamethasone at 37°C through CFP filters, allowing selective excitation of the donor without significant cross talk between donor and acceptor. Sequences of 1 s exposure were optimal to collect a sufficient number of data points in the regions of the curve with maximal slope variation. The data are recorded as a time stack of images. The results obtained by pbFRET are only moderately sensitive to the variation of fluorescence signals of the donor fluorophore (Figure S2). We checked for (and excluded) donor photoisomerization by collecting 1 s images every 30 s after the end of the photobleaching routine.

We picked eight 400-pixel ROIs in each nucleus, avoiding nucleoli where GR is excluded. The mean fluorescence intensity in each ROI was extracted from the time stack automatically via IQARO (image quantitative analysis routine), described at http://www.bmsc.washington.edu/raster3d/), a web-based software application we developed to handle images in "Raster 3D" format. This binary format is used to store a stack of images in a single file, which stores metainformation about the whole stack (including the number of images in the stack, their ordering, and their dimensions). A 2-byte number, proportional to its intensity level, represents each pixel. The images stored in a stack are indexed along three independent axes as a maximum, determined by the image acquisition procedure: the z-axis, the t-axis, and the wavelength, and plotted against time after internal normalization.

After background correction, photobleaching kinetics are best fitted by a double exponential equation:

$$I(t) = I_0 + I_1 e^{-k_1 t} + I_2 e^{-k_2 t} \quad (1)$$

where I(t) is the mean fluorescence intensity in each region of interest (ROI) at each time point; k_1 and k_2 are the rate constants and I_1 and I_2 are the amplitudes of the first and the second phase of the decay; I_0 is the residual fluorescence intensity. Fluorescence I(t) starts at ($I_1 + I_2 + I_0$) and decays to I_0 with rate constants k_1 and k_2.

To correct for the residual fluorescence (I_0, as extrapolated from Equation 1) and for the variation in the initial fluorescence intensity, an internal normalization of I(t) is applied for which $I(t_{max}) = 1$ and $I_0 = 0$. Equation 1 is then recast as:

$$I'(t) = I'_1 e^{-k_1 t} + I'_2 e^{-k_2 t} \quad (2)$$

where the half-lives characterizing the two-phase decay are $t_1 = 0.69/k_1$ and $t_2 = 0.69/k_2$.

Nonlinear regression fittings were obtained by sum-of-squares minimization with initial value estimates and convergence criteria to less than 0.01%.

Within the same nucleus, we did not observe large differences among photobleaching kinetics of the randomly chosen ROIs. Therefore, we can treat the readings on different ROIs in the same cells as replicates and compute an average photobleaching kinetics for each nucleus; the standard errors on the fitted curves encapsulate the variability within each cell.

The complexities arising from the presence of two different rate constants, k_1 and k_2, can be reduced by considering an amplitude-weighted average of the two rate constants:

$$t_{eff} = I'_1 t_1 + I'_2 t_2 \quad (3)$$

Despite the variability of donor expression in transiently transfected cells, photobleaching kinetics was comparable from cell to cell and in different experiments. Thus, averages over populations of cells can be calculated. Statistical analysis was performed using one-way analysis of variance (ANOVA) and applying Bonferroni's Multiple Comparison Test for selected pairs of groups (Altman and Bland, 1996; Bland and Altman, 1995).

FRET efficiency (%) in single cells is calculated as:

$$E^{\%}_{FRET} = \left(1 - \frac{t^D_{eff}}{t^{DA}_{eff}}\right) 100 \quad (4)$$

where t^D is the mean photobleaching time of the donor, and t^{DA} is the photobleaching time of the donor in the presence of acceptor. Cells whose t^{DA} is within the standard error of the donor alone t^D have a FRET efficiency not statistically different from 0 and can be considered not to respond to FRET. In our experiments, nonresponders often accounted for about 20% of the total cell population examined.

Each experiment was repeated at least three times, although generally only one experiment is reported in each figure.

Confocal Imaging

Cells were grown in glass-bottom petri dishes (LabTek, Nunc), transfected, and stimulated. Stacks of images were acquired at 37°C on a Leica TCS SP2 AOBS confocal microscope with a 63×/1.4 N.A. oil immersion objective and 5× zoom (512 × 512 pixels; voxel size 0.066 × 0.066 × 0.03 μm). The bright fluorescent cluster of GREs (where present) was the central image in the stack.

Fluorescence Recovery after Photobleaching (FRAP)

Photobleaching experiments were performed on a Leica TCS SP2 AOBS confocal microscope equipped with a 63×/1.4 N.A. oil immersion objective at 37°C. To define the prebleaching plateau, five single-section 12-bit images were acquired with 5× zoom on a small area (47 × 12 μm, pixel size 0.093 μm) to maximize acquisition speed (108 ms/frame). Bleaching was performed with four 108 ms pulses using the 488 nm and 514 nm lines of an Ar laser (100 mW nominal output) at 90% power on a 1 μm radius area. Fluorescence recovery was monitored collecting 150 single-section images at 108 ms intervals with low laser intensity (2% of the bleach intensity with the single 488 nm laser line, detection 520–650 nm). For quantitative analysis of fluorescence recovery, data were doubly normalized as described by Phair et al. (2004a). Each experiment was repeated at least twice.

ATP Depletion

Cells transfected and cultured in glucocorticoid-depleted medium were stimulated with 100 nM dexamethasone for 15 min, and they were ATP-depleted as described by Stavreva et al. (2004) by incubation for 30 min in glucose-free DMEM containing 1% glucocorticoid-depleted FCS, 100 nM dexamethasone, 6 mM 2-deoxyglucose, 10 mM Na azide, and 20 mM HEPES. FRAP data were collected within 30 min from ATP depletion.

Proteasome and Chaperone Inhibition

Transfected MEFs cultured in glucocorticoid-depleted medium were treated with 10 μM MG-132 (Calbiochem) for 2 hr, stimulated with 100 nM dexamethasone for 15 min, and then subjected to FRAP analysis. Alternatively, transfected MEFs were stimulated with 100 nM dexamethasone for 30 min, then treated with 2.5 μg/ml geldanamycin (Calbiochem) for 30 min, and subjected to FRAP analysis.

Supplemental Data

Supplemental Data include four additional figures and can be found with this article online at http://www.molecule.org/cgi/content/full/18/1/109/DC1/.

Acknowledgments

We thank especially J. McNally for providing the cells with the MMTV array and for important comments and suggestions. T. Rossi, E. Spoldi, and S. Deceglie helped in generating the reagents and in data analysis; J. Swedlow and A. Lamond introduced us to fluorescence microscopy; M. Bustin, T. Grange, H. Kimura, T. Misteli, M. Vigneron, and O. Wrange provided reagents; and the ALEMBIC facility staff contributed assistance. We thank G. Natoli and the members of the Bianchi lab for discussions. This work was supported by grants from the Italian Ministry of Education, University, and Research to M.E.B., A.A., and V.R.C.

Received: September 28, 2004
Revised: January 14, 2005
Accepted: March 8, 2005
Published: March 31, 2005

References

Agalioti, T., Lomvardas, S., Parekh, B., Yie, J., Maniatis, T., and Thanos, D. (2000). Ordered recruitment of chromatin modifying and general transcription factors to the IFN-β promoter. Cell *103*, 667–678.

Agresti, A., and Bianchi, M.E. (2003). HMGB proteins and gene expression. Curr. Opin. Genet. Dev. *13*, 170–178.

Altman, D.G., and Bland, J.M. (1996). Comparing several groups using analysis of variance. BMJ *312*, 1472–1473.

Becker, M., Baumann, C., John, S., Walker, D.A., Vigneron, M., McNally, J.G., and Hager, G.L. (2002). Dynamic behavior of transcription factors on a natural promoter in living cells. EMBO Rep. *3*, 1188–1194.

Belikov, S., Gelius, B., and Wrange, O. (2001). Hormone-induced nucleosome positioning in the MMTV promoter is reversible. EMBO J. *20*, 2802–2811.

Bland, J.M., and Altman, D.G. (1995). Multiple significance tests: the Bonferroni method. BMJ *310*, 170.

Bonaldi, T., Talamo, F., Scaffidi, P., Ferrera, D., Porto, A., Bachi, A., Rubartelli, A., Agresti, A., and Bianchi, M.E. (2003). Monocytic cells hyperacetylate chromatin protein HMGB1 to redirect it towards secretion. EMBO J. *22*, 5551–5560.

Boonyaaratanakornkit, V., Melvin, V., Prendergast, P., Altmann, M., Ronfani, L., Bianchi, E.M., Tarasaviciene, A., Nordeen, S.K., Allegretto, E.A., and Edwards, D.P. (1998). High mobility group chromatin proteins -1 and -2 functionally interact with steroid hormone receptors to enhance their DNA binding in vitro and transcriptional activity in mammalian cells. Mol. Cell. Biol. *18*, 4471–4487.

Calogero, S., Grassi, F., Aguzzi, A., Voigtländer, T., Ferrier, P., Ferrari, S., and Bianchi, M.E. (1999). The lack of chromosomal protein HMG1 does not disrupt cell growth, but causes lethal hypoglycaemia in newborn mice. Nat. Genet. *22*, 276–280.

Carey, M. (1998). The enhanceosome and transcriptional synergy. Cell *92*, 5–8.

Chattoraj, M., King, B.A., Bublitz, G.U., and Boxer, S.G. (1996). Ultra-fast excited state dynamics in green fluorescent protein: multiple states and proton transfer. Proc. Natl. Acad. Sci. USA *93*, 8362–8367.

Clegg, R.M. (1996). Fluorescence Resonance Energy Transfer. In Fluorescence Imaging Spectroscopy and Microscopy,, X.F. Wang and B. Herman, eds. (New York: John Wiley & Sons, Inc.), pp. 179–236.

Elbi, C., Walker, D.A., Romero, G., Sullivan, W.P., Toft, D.O., Hager, G.L., and DeFranco, D.B. (2004). Molecular chaperones function as steroid receptor nuclear mobility factors. Proc. Natl. Acad. Sci. USA *101*, 2876–2881.

Ellwood, K.B., Yen, Y.M., Johnson, R.C., and Carey, M. (2000). Mechanism for specificity by HMG-1 in enhanceosome assembly. Mol. Cell. Biol. *20*, 4359–4370.

Fletcher, T.M., Xiao, N., Mautino, G., Baumann, C.T., Wolford, R., Warren, B.S., and Hager, G.L. (2002). ATP-dependent mobilization of the glucocorticoid receptor during chromatin remodeling. Mol. Cell. Biol. *22*, 3255–3263.

Freeman, B.C., and Yamamoto, K.R. (2002). Disassembly of transcriptional regulatory complexes by molecular chaperones. Science *296*, 2232–2235.

Giavara, S., Kosmidou, E., Hande, M.P., Bianchi, M.E., Morgan, A., d'Adda di Fagagna, F., and Jackson, S.P. (2005). Yeast Nhp6A/B and mammalian Hmyb1 facilitate the maintenance of genome stability. Curr. Biol. *15*, 68–72.

Htun, H., Barsony, J., Renyi, I., Gould, D.L., and Hager, G.L. (1996). Visualization of glucocorticoid receptor translocation and intranuclear organization in living cells with a green fluorescent protein chimera. Proc. Natl. Acad. Sci. USA *93*, 4845–4850.

Jovin, T.M., and Arndt-Jovin, D.J. (1989). Luminescence digital imaging microscopy. Annu. Rev. Biophys. Biophys. Chem. *18*, 271–308.

Kimura, H., and Cook, P.R. (2001). Kinetics of core histones in living human cells: little exchange of H3 and H4 and some rapid exchange of H2B. J. Cell Biol. *153*, 1341–1353.

Lomvardas, S., and Thanos, D. (2001). Nucleosome sliding via TBP binding in vivo. Cell *106*, 685–696.

McNally, J.G., Muller, W.G., Walker, D., Wolford, R., and Hager, G.L. (2000). The glucocorticoid receptor: rapid exchange with regulatory sites in living cells. Science *287*, 1262–1265.

Melvin, V.S., Roemer, S.C., Churchill, M.E., and Edwards, D.P. (2002). The C-terminal extension (CTE) of the nuclear hormone receptor DNA binding domain determines interactions and functional response to the HMGB-1/-2 co-regulatory proteins. J. Biol. Chem. *277*, 25115–25124.

Merika, M., and Thanos, D. (2001). Enhanceosomes. Curr. Opin. Genet. Dev. *11*, 205–208.

Misteli, T. (2001). Protein dynamics: implications for nuclear architecture and gene expression. Science *291*, 843–847.

Misteli, T., Gunjan, A., Hock, R., Bustin, M., and Brown, D.T. (2000). Dynamic binding of histone H1 to chromatin in living cells. Nature *408*, 877–881.

Muller, W.G., Walker, D., Hager, G.L., and McNally, J.G. (2001). Large-scale chromatin decondensation and recondensation regulated by transcription from a natural promoter. J. Cell Biol. *154*, 33–48.

Munshi, N., Agalioti, T., Lomvardas, S., Merika, M., Chen, G., and Thanos, D. (2001). Coordination of a transcriptional switch by HMGI(Y) acetylation. Science *293*, 1133–1136.

Nagaich, A., Walker, D., Wolford, R., and Hager, G. (2004). Rapid periodic binding and displacement of the glucocorticoid receptor during chromatin remodeling. Mol. Cell *14*, 163–174.

Pallier, C., Scaffidi, P., Chopineau-Proust, S., Agresti, A., Nordmann, P., Bianchi, M.E., and Marechal, V. (2003). Association of chromatin proteins HMGB1 and HMGB2 with mitotic chromosomes. Mol. Biol. Cell *14*, 3414–3426.

Patterson, G.H., Piston, D.W., and Barisas, B.G. (2000). Forster distances between green fluorescent protein pairs. Anal. Biochem. *284*, 438–440.

Perlmann, T., and Wrange, O. (1988). Specific glucocorticoid receptor binding to DNA reconstituted in a nucleosome. EMBO J. *7*, 3073–3079.

Phair, R.D., Gorski, S.A., and Misteli, T. (2004a). Measurement of dynamic protein binding to chromatin in vivo, using photobleaching microscopy. Methods Enzymol. *375*, 393–414.

Phair, R.D., Scaffidi, P., Elbi, C., Vecerova, J., Dey, A., Ozato, K., Brown, D.T., Hager, G., Bustin, M., and Misteli, T. (2004b). Global nature of dynamic protein-chromatin interactions in vivo: three-dimensional genome scanning and dynamic interaction networks of chromatin proteins. Mol. Cell. Biol. *24*, 6393–6402.

Reichardt, H.M., Kaestner, K.H., Tuckermann, J., Kretz, O., Wesserly, O., Bock, R., Gass, P., Schmid, W., Herrlich, P., Angel, P., and Schütz, G. (1998). DNA binding of the glucocorticoid receptor is not essential for survival. Cell *93*, 531–541.

Scaffidi, P., Misteli, T., and Bianchi, M.E. (2002). Release of chromatin protein HMGB1 by necrotic cells triggers inflammation. Nature *418*, 191–195.

Schaaf, M.J., and Cidlowski, J.A. (2003). Molecular determinants of glucocorticoid receptor mobility in living cells: the importance of ligand affinity. Mol. Cell. Biol. *23*, 1922–1934.

Sekar, R.B., and Periasamy, A. (2003). Fluorescence resonance energy transfer (FRET) microscopy imaging of live cell protein localizations. J. Cell Biol. *160*, 629–633.

Stavreva, D.A., Muller, W.G., Hager, G.L., Smith, C.L., and McNally, J.G. (2004). Rapid glucocorticoid receptor exchange at a promoter

is coupled to transcription and regulated by chaperones and proteasomes. Mol. Cell. Biol. *24*, 2682–2697.

Thomas, J.O., and Travers, A.A. (2001). HMG1 and *2*, and related 'architectural' DNA binding proteins. Trends Biochem. Sci. *26*, 167–174.

Tsien, R.Y. (1998). The green fluorescent protein. Annu. Rev. Biochem. *67*, 509–544.

Young, R.M., Arnette, J.K., Roess, D.A., and Barisas, B.G. (1994). Quantitation of fluorescence energy transfer between cell surface proteins via fluorescence donor photobleaching kinetics. Biophys. J. *67*, 881–888.